Research Article

Health Monitoring of Automotive Suspensions: A LSTM Network Approach

Haoju Hu, Huan Luo ⓘ, and Xiaoqiang Deng

GAC Automotive Research & Development Center, Guangzhou 511434, China

Correspondence should be addressed to Huan Luo; luohuan616@163.com

In the automotive industry, one of the critical issues is to develop a health monitoring system for condition assessment and remaining fatigue life estimation of key load-bearing components including automotive suspension. However, considering the difficulty to obtain expert knowledge and nonlinear dynamics in large-scale sensory data, health monitoring of automotive suspension is a challenging work. With the development of deep learning based sequence models in recent years, a long short-term memory (LSTM) network has been proved to capture long-term dependencies in time-series prediction without additional expert knowledge. In this paper, a novel health monitoring system based on a LSTM network is proposed to estimate the remaining fatigue life of automotive suspension. Specifically, first durability tests under various driving cycles are implemented to obtain sequential sensory data provided by common sensors on a test car. Then, a LSTM-based load identification method is designed to predict dynamic stress histories based on the available sensory data. Finally, the damages and remaining fatigue life of the suspensions are estimated by each time step. The experimental results prove that our model can achieve a better performance compared with other representative models.

1. Introduction

Structural health monitoring is becoming important for condition assessment and future performance predictions of critical load-bearing components in the automotive industry [1, 2]. A well-designed monitoring system, assessing structure integrity and predicting remaining fatigue life in real time, can provide efficient inspection and improvement plans in both automotive durability and lightweight design in [3]. As one of the most critical load-bearing components in cars, automotive suspension is subjected to various loads under operating conditions and may suffer from significant damage. Therefore, there is a stringent need to develop a health monitoring system for the estimation of remaining fatigue life and warn of required schedule to avoid failure.

In recent years, extensive research has been conducted in structural health monitoring. According to the distinct damage identification methods, existing health monitoring systems can be divided into two categories: model-based approaches and data-driven ones.

In the former case, the degradation process is identified based on experimental response data from structures such as fracture length and nature frequency [4–7]. The experimental response data are usually collected by complicated instruments usually applied to large machinery. In addition, the performance of model-based approaches heavily depends on the expert knowledge that is often unavailable in practical applications. As a result, model-based approaches are not suitable to be applied in series-production cars for their high cost and uncertainty.

In the latter case, modeling the evolution of the degradation process relies on processing history data based on a detailed numerical model. Many researchers have make efforts to devise reliable data-driven approaches in health monitoring system, such as Extended Kalman Filter (EKF) [8, 9], Back Propagation (BP) neural network [10–12], particle filtering (PF) [13], Gaussian Process Regression (GPR) [14], Support Vector Machine (SVM) [15], recurrent neural networks (RNNs) [16], and the combination of these algorithms [17], wherein the numerical model can map high

dimensional and nonlinear relationship as well as predicting the health status in real time without prior assumptions. Additionally, with the improvement in sensors and computer system, data-driven monitoring system becomes preferred. Consequently, this work focuses on the data-driven approaches for monitoring the actual level of damage of automotive suspension.

The core step of data-driven monitoring systems is to estimate the dynamic loads from sequential sensory data. Among previous data-driven approaches, the neural network approaches are not sequential models. They cannot capture the sequential characteristics in the large-scale sensory data, leading to poor predicted results. Except for neural network approaches, other data-driven approaches based on sequential models, including EKF and PF, are suitable for addressing sequential data.

Foulard et al. [18] developed an online and real-time monitoring method for remaining service life estimation of automotive transmission, which can represent the state of the art in the automotive industry. In this monitoring method, an observer-based torque identification method relying on an EKF is addressed to estimate damage of transmission under real driving conditions. But the limited use of EKF in nonlinear system and the inability of an EKF to capture long-term dependencies affect the universality and accuracy of this approach. For the fast development of data measuring and data transmission technology, a huge amount of vehicle vibration signals in real time can be obtained by sensors nowadays. These tremendous vibration signals facilitate a more accurate damage prognosis results. Therefore, improving the prognosis accuracy by using available vibration signals is a promising research direction in developing a health monitoring system.

Most aforementioned data-driven identification methods are restricted in searching the shallow correlation within the limited data, which cannot penetrate deep correlation and implicit load information [19]. With the fast development of artificial intelligence in recent years, especially deep learning and recurrent neural network, modeling complex nonlinear relationship with advanced learning approaches has become a new trend [20]. A long short-term memory (LSTM) network, which is originally introduced for sequence learning, is able to cope with the complex correlation within time series in long time term [21–24]. In near several years, LSTM networks have been applied to capture nonlinear dynamics in time-series sensory data [25–30]. In these researches, the LSTM network has obviously higher performance than traditional data-driven approaches. The results in their studies suggest that this advanced machine learning approach deserves to be considered a new effective tool in the specific task of monitoring the health status of automotive suspensions.

However, the researchers in [25–30] tested their LSTM networks through test rig under laboratory conditions or specific working condition. Therefore, they mainly focused on theoretical analysis. However, due to complex vibration loads under real operation conditions, it is far from an easy work to conduct a practical application for LSTM-based technologies. To validate the superiority and practicability of LSTM networks, our health monitoring system is applied to an automotive suspension component under real operation conditions.

In this paper, we propose an applicative approach to develop a health monitoring system for estimating remaining fatigue life of automotive suspensions. In the proposed health monitoring system, firstly, durability tests are implemented to collect sensory data for building database of the monitoring system. The sensory data contain two types of signals: vibration signals and fatigue loads. Then, a LSTM-based fatigue load identification method is developed to capture the nonlinear relationship between the vibration signals and fatigue loads in terms of stress histories. Finally, the well-trained LSTM network predicts current fatigue loads from real-time measurement values of vibration signals. Based on the predicted fatigue loads, the damage condition and remaining fatigue life of the component are calculated. The performance of the proposed approach is validated by comparative analyses of the estimated damage results with different methods. As the automotive technology advance, vehicles are equipped with more and more sensors, an important part of which is to measure some vibration signals for monitoring and controlling the cars. Therefore, the proposed approach provides a new strategy for developing an applicative health monitoring system in series-production cars.

This paper is organized as follows. In Section 2, the adopted flowchart for the monitoring system development is overviewed. In Section 3, details of tests to collect sensor-based signals and the damage calculation model are described. In Section 4, the proposed LSTM-based load identification method is presented. Section 5 shows the estimated results of damage condition. In Section 6, the conclusions and the perspectives are presented.

2. Overview of the Proposed Approach for Remaining Fatigue Life Estimation of Automotive Suspensions

The proposed approach is aimed at developing an applicative health monitoring system for estimating the remaining fatigue life of automotive suspensions. As illustrated in Figure 1, it consists of three main modules: data collection, fatigue load identification, and damage prognosis.

Firstly, as a data-driven study on developing a health monitoring system, a set of sample data are needed to be collected. The data collection should be carefully implemented to make sure that the samples data are accurate, comprehensive, and discriminative. Following this guideline, durability tests under various driving cycles are implemented. In the tests, two types of signals are collected by sensors, vibration signals and fatigue loads. The vibration signals are measured by common sensors in series-production cars, such as accelerometer and gyroscope. The fatigue loads are measured by sensors only equipped in testing phase, such as strain rosette.

Then, the collected sensory data are then processed in the second module of the framework. The fatigue load
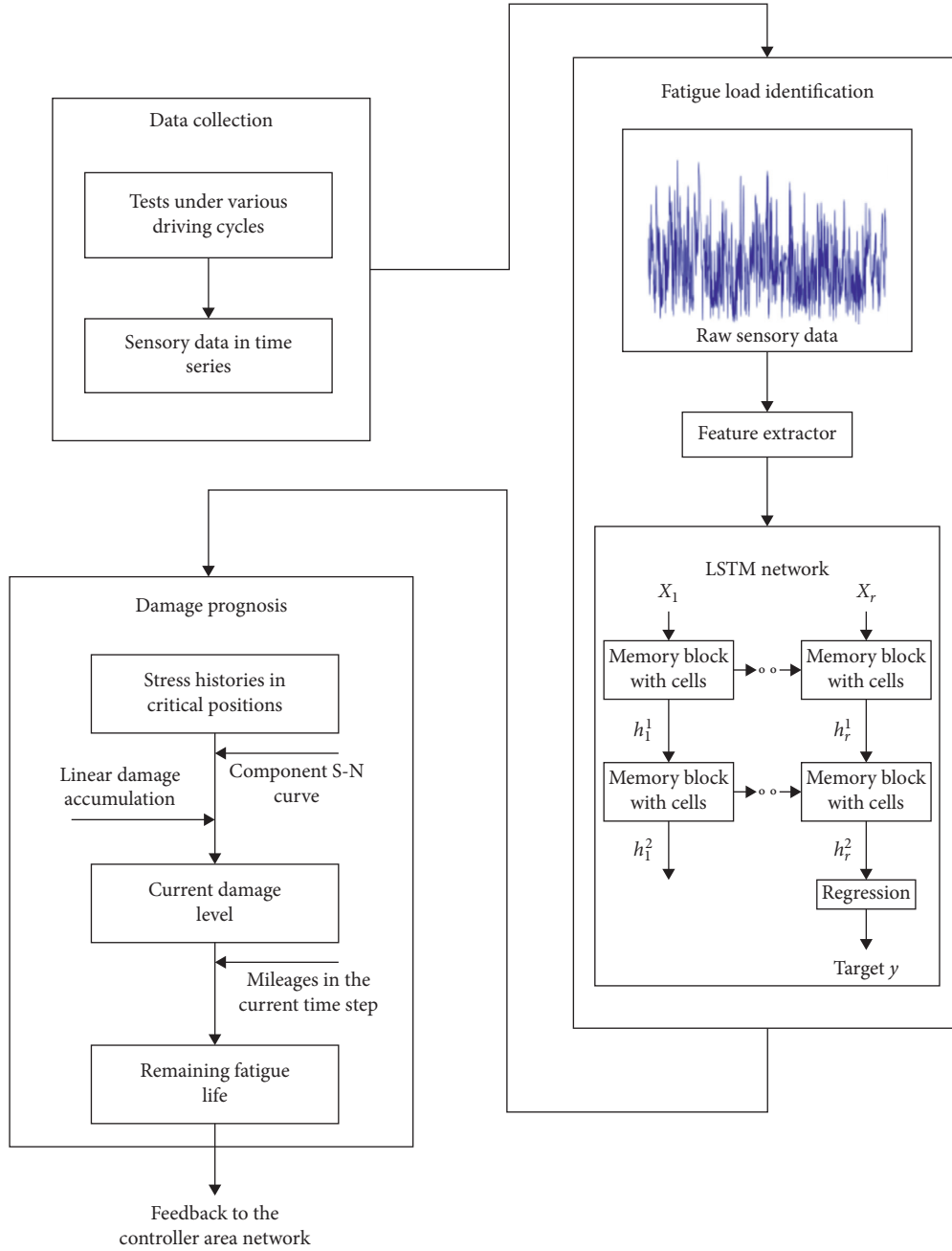
FIGURE 1: Adopted flowchart to develop a structural health monitoring system.

identification works as the core part of the monitoring system, which can capture the nonlinear relationship between the vibration signals and fatigue loads from historical data as well as predicting corresponding fatigue loads from real-time measured vibration signals.

Finally, the damage prognosis module uses reliable damage calculation model to compute the damage level of the automotive suspensions and corresponding remaining fatigue life. Once the predefined threshold for the component reliability is exceeded, the system sends alarm maintenance signals.

3. Sensory Data Collection and Damage Calculation Models

The health monitoring of automotive suspensions involves dynamics events such as operation processes for different road profiles, wheel dynamics, and body vibrations. In addition, it involves nonlinearity such as large deformation at extreme operation conditions [31]. Therefore, the torsion beam suspension model can serve as reference, considered as representative of the real automotive nonlinear dynamics. There are seven main welded parts in the torsion beam

suspension (see Figure 2). Table 1 shows the material properties for each part of the components obtained from the manufacturer. As the key load-bearing component in a vehicle, the torsion beam suspension is subjected to complex variable loads under service loads, vulnerable to damage.

The aforementioned data-driven approach is adopted in the monitoring system. In this regard, data collection is of great importance. Although using a simulation model is a growing trend in automotive engineering for its low cost and high efficiency, it is still difficult to achieve accurate dynamic loads by simulation techniques, allowing for nonlinearity [32] and large data length. Under this consideration, various durability tests are implemented for data collection. The main contents of the experimental works consist of two aspects. The first is to specify the driving cycles that can reflect real operation conditions. The second is to specify the measured signals in the sample data. Theses aspects are addressed in the following subsections, respectively.

3.1. Driving Cycles. To make the monitoring system effective, various driving cycles, which should cover real operation conditions as many as possible, are selected in the process of bench tests and road tests. The bench tests are performed to obtain data set for training and testing the LSTM model in fatigue load identification method. After establishment, the LSTM model is validated by error analysis of the predicted fatigue loads from measured vibration signals in road tests.

The reason for not using road tests to collect all data set is justified in two essential aspects. Firstly, it is of high cost and time consuming to drive the vehicle on all the necessary driving cycles. Secondly, the reproducibility of the tests will not be ensured, which is of great importance to the results.

Three continuous factors of operating conditions are varied in driving cycles: road profile, additional load, and driving speed. In the bench tests (see Figure 3), the selected driving cycles consist of 20 road profiles. These profiles are divided into two types: the first type, called standard road profile, consists of 6 reconstructed road profiles based on international road standard (class A-F) [33]. The second type, called proving ground road profile, consists of 14 road profiles obtained from Xiangyang automotive proving ground (Belgian, disrepair, railway, small bump, pebble, washboard, fish scale, twist, big bump, speed bump, resonance, sandstone, brake, and long wave).

In the road tests, the vehicle runs on different types of road (country road, pavement, and highway) with different speeds and additional loads. As some driving cycles lead to small fatigue loads, they cause a minor impact on damage calculation of the suspensions and share a small proportion in the whole driving cycles of various factor combinations. It means that most of the combinations of low speed, small additional load, and smooth road profile are neglected in this work. The car mass of the experimental vehicle, equipped with the reference suspension, is about 1200 kg for a maximal power of 92.6 kw. The range of the additional load is from 60 to 500 kg. The range of the speed refers to the test specifications of the proving ground and traffic laws. As an example, the speed is limited in the range from 60 to 120 km/
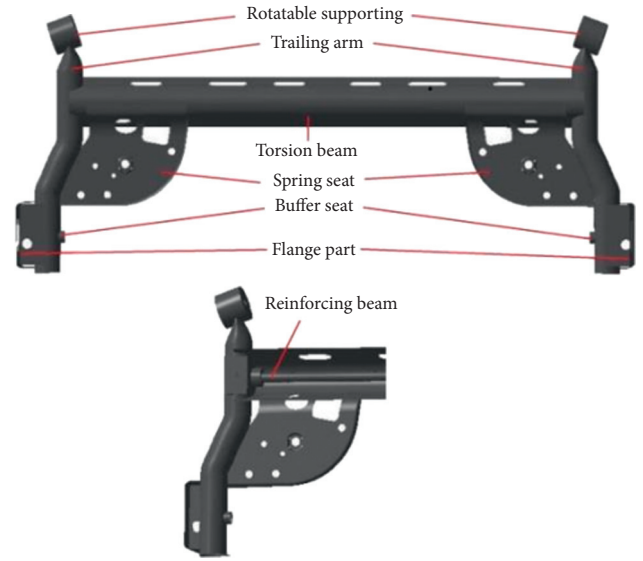

Figure 2: Target torsion beam rear suspension.

h on a China's highway (class A-C). All the combinations in the bench tests are presented in Table 2. The selection of the combinations of operation conditions refers to [6]. All the tests in our experiments are implemented according to motor vehicle durability running test method [34].

3.2. Measured Signals. The vibration signals, having effects on the damages calculation of the automotive suspension, are measured as referred signals in experimental tests. As the monitoring system is developed for its application to series-production vehicle, the available signals on the Controller Area Network (CAN) of a standard vehicle have to be taken into consideration. For the sake of generality, available signals are measured by common sensors: the displacement and angular velocity of vehicle body in the x, y, and z direction, the deformation of two springs and two shock absorbers in the rear torsion beam suspension, the deformation of the two springs in the Macpherson front suspension, and the vertical acceleration of the four spindles in the center of wheels. Though fewer signals may be needed in this monitoring system by feature selection for signals from simulation model, sixteen measured signals are considered to store information for developing potentially promising method from a long-term perspective.

In the experimental tests, we measure the stress histories in critical positions that act as goal values during the process of designing the architectures of the supervised-learning LSTM network. The stress histories are only measured in the stage of the monitoring system development, estimated by using the well-trained LSTM network in the stage of monitoring system application. The critical positions for fixing strain gauges (45-degree internal angle of rosette) are chosen based on simulation model and practical cases (see Figure 4) [35]. It is clear that the critical positions are located in welded connections.

During the road tests, all test equipment has been strictly inspected to ensure its good condition, including the strain

TABLE 1: Material properties for each part of the torsion beam suspension.

	Rotatable supporting	Trailing arm	Torsion beam	Spring seat	Buffer seat	Flange part	Reinforcing beam
Thickness (mm)	Solid	4	4.5	4	10	6	Solid
Ultimate tensile strength (MPa)	440	550	568	550	470	510	537
Yield strength (MPa)	235	345	432	430	310	416	305
Elasticity modulus (MPa)	2.07E5	2E5	2E5	2E5	2E5	2E5	2.07E5
Fatigue strength coefficient (MPa)	2144	917	950	917	570	421	1517
Fatigue strength exponent	−0.179	−0.095	−0.095	−0.095	−0.09	−0.09	−0.14

FIGURE 3: Bench test.

TABLE 2: All the driving cycles in the bench tests.

RP	AL	S	T	RP	AL	S	T	RP	AL	S	T	RP	AL	S	T	RP	AL	S	T
A	60	100	30	B	60	90	30	C	60	80	30	D	60	50	60	E	60	20	60
A	60	120	30	B	60	110	30	C	60	100	30	D	60	60	60	E	60	30	60
A	300	80	30	B	200	100	30	C	200	90	30	D	200	50	60	E	200	20	60
A	300	100	30	B	300	90	30	C	300	80	30	D	300	50	60	E	300	10	60
A	300	120	30	B	300	110	30	C	300	100	30	D	300	60	60	E	300	20	60
A	500	80	30	B	500	70	30	C	500	60	30	D	500	40	60	E	500	10	60
A	500	100	30	B	500	90	30	C	500	80	30	D	500	50	60	E	500	20	60
RP	AL	S	T	RP	AL	S	T	RP	AL	S	T	RP	AL	S	T	RP	AL	S	T
F	60	20	60	Di	60	45	60	Ra	400	40	60	Pe	400	30	60	Fi	300	40	60
F	60	30	60	Di	200	35	60	SB	60	35	60	Pe	500	20	60	Fi	400	30	60
F	200	20	60	Di	300	30	60	SB	100	35	60	Wa	60	50	60	Fi	500	20	60
F	300	10	60	Di	500	20	60	SB	300	30	60	Wa	200	40	60	Tw	300	10	60
F	300	20	60	Ra	60	45	60	SB	500	20	60	Wa	300	30	60	Tw	500	10	60
F	500	10	60	Ra	300	30	60	Pe	60	50	60	Wa	500	20	60	BB	60	25	60
F	500	20	60	Ra	500	15	60	Pe	300	40	60	Fi	60	50	60	BB	300	20	60
RP	AL	S	T	RP	AL	S	T	RP	AL	S	T	RP	AL	S	T				
BB	400	15	60	Sp	300	50	60	Sa	60	30	60	Br	500	10	60				
BB	500	10	60	Sp	400	40	60	Sa	300	20	60	Lo	60	45	60				
Be	60	20	60	Sp	500	35	60	Sa	400	15	60	Lo	200	40	60				
Be	200	15	60	Re	60	30	60	Sa	500	10	60	Lo	300	30	60				
Be	300	15	60	Re	200	25	60	Br	60	30	60	Lo	500	20	60				
Be	500	10	60	Re	300	20	60	Br	300	20	60								
Sp	60	60	60	Re	500	10	60	Br	400	15	60								

RP: road profile AL: additional load (kg) S: speed (km/h) T: duration of the test (second)
A-F: class of international road standard
Di: disrepair Ra: railway SB: small bump Pe: pebble Wa: washboard Fi: fish scale
Tw: twist BB: big bump Be: Belgian
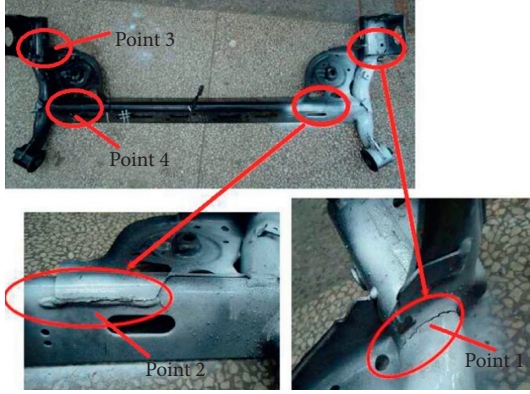Sp: speed bump Re: resonance Sa: sand stone Br: brake Lo: long wave

FIGURE 4: Measuring points of the automotive suspension.

FIGURE 5: Adopted damage calculation model.

gauges and data acquisition equipment. Then, the measured vibration signals and strain signals are amplified, filtered, transferred to digitals, and then imported to computer analysis system in the sampling frequency of 500 Hz during the tests. The stress histories can be calculated with the following formula:

$$
\frac{\sigma_1}{\sigma_2} = \frac{E}{2} \left[\frac{\varepsilon_0 + \varepsilon_{90}}{1 - \mu} \left(\pm \right) \frac{\sqrt{2}}{1 + \mu} \sqrt{\left(\varepsilon_0 - \varepsilon_{45} \right)^2 + \left(\varepsilon_{45} - \varepsilon_{90} \right)^2} \right],
$$

$$
\tau_{\max} = \frac{\sqrt{2}E}{1 + \mu} \sqrt{\left(\varepsilon_0 - \varepsilon_{45} \right)^2 + \left(\varepsilon_{45} - \varepsilon_{90} \right)^2},
$$

$$(1)$$

where Young modulus E is 2.07×10^5 MPa, Poisson ratio is μ 0.27, $\varepsilon_0, \varepsilon_{45},$ and ε_{90} are measured strain signals from each strain rosette, respectively, σ_1 and σ_2 are two principal stresses, and τ_{max} is the maximum shear stress.

In consideration of analytical efficiency, the data set collected from bench tests is preprocessed by extracting partial data representing each driving cycle and reducing the sampling frequency to 100 Hz. The details of the pre-processing step can be found in [18, 36]. In this work, the total number of extracted sequential data is about 120 thousands. Then, these extracted data are divided into two sets, a training data set and a test data set (that is not a subset of the training set). As the data set is time-series signal, the dynamic response at a time step may be related to current inputting loads and previous inputting loads. As a result, K-fold cross-validation is not a suitable method used to divide the extracted data. The first 80 percent of signals in each driving cycle are selected as training data set with the rest of signals as test data set. The collected sequential data in road tests are also preprocessed by frequency decrease, and their total number is about 50 thousands.

3.3. Damage Calculation Model.

The normal stress method, in combination of linear damage accumulation method (Palmgren-Miner rule) and rain-flow counting method, is considered for the damage calculation in the health moni-toring system [37]. The model for damage calculation and remaining fatigue life estimation is presented in Figure 5. W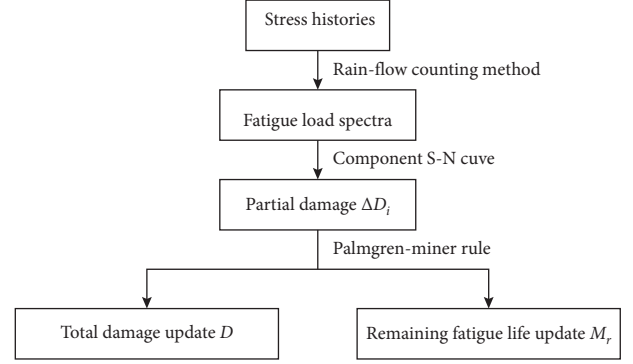e update the partial damage ΔD_i, the total damage D, and remaining fatigue life indicted by remaining mileages M_r in the critical positions every minute using the following functions:

$$
N_j = \left(\frac{\Delta \sigma_j}{S_f} \right)^{(1/b)},
$$

$$
\Delta D_i = \sum_j \frac{n_j}{N_j}, D = \sum_i \Delta D_i, M_r \approx \left(\frac{D_T}{D} - 1 \right) * M_i,
$$

$$(2)$$

where the spectrum of stress ranges $\Delta \sigma_j$ and associated number of counted cycles n_j for the current time step are calculated by rain-flow counting method. The material properties parameters (S_f and b) for each part of the components are obtained from the manufacturer. N_j is the number of cycles to failure at each stress range; D_T is the total damage as the component fails; M_i is the mileages in the current time step.

4. Fatigue Load Identification

The challenge of developing a health monitoring system lies in proposing an accurate and easily implementable fatigue load identification method. As the signals in the monitoring system are in the form of continuous time-series data, a dynamic neural network dealing with time sequential inputs is suitable. For this reason, a recurrent neural network named LSTM network is adopted.

4.1. Structure of LSTM Network.

The primary objectives of LSTM network are to model long-term dependencies and determine the correlation for time-series problems. These features are desirable for fatigue load identification. In the structure of a LSTM network, it uses special hidden units called memory cells to remember input for a long time, which is the key for its application in time-series analysis. Figure 6 illustrates a single memory cell. The model input is known data denoted as X_t with the output of the forecast result denoted as Y_t. In the context of fatigue load identi-fication, X represents measured vibration signals and Y the stress histories in one of the critical positions. There are three gates in the memory cell, namely, input gates, forget gates, and output gates. Moreover, the state of the cell is indicated
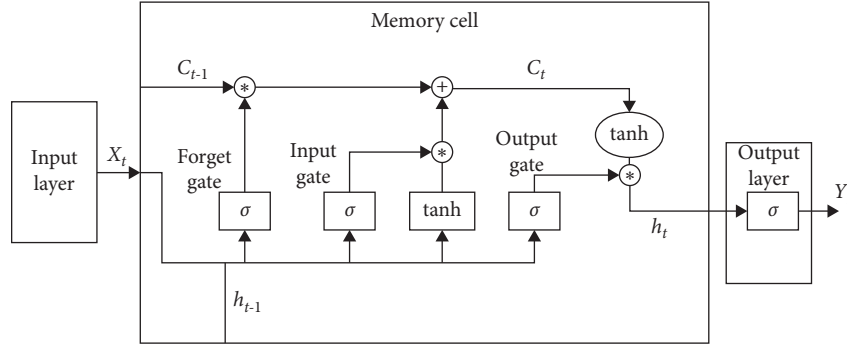
FIGURE 6: Memory cell of a LSTM network.

by C_t. As the information flow in the structure of memory cell, the state and output updates can be implemented by the following functions:

$$f_t = \sigma\left(W_{xf}X_t + W_{hf}h_{t-1} + b_f\right),$$
$$i_t = \sigma\left(W_{xi}X_t + W_{hi}h_{t-1} + b_i\right),$$
$$C_t = f_t * C_{t-1} + i_t * \tanh\left(W_{xc}X_t + W_{hc}h_{t-1} + b_c\right),$$
$$o_t = \sigma\left(W_{xo}X_t + W_{ho}h_{t-1} + b_o\right),$$
$$h_t = o_t * \tanh\left(C_t\right),$$
$$Y_t = \sigma\left(W_{hy}h_t + b_y\right),$$

(3)

where ' $*$ ' is scalar product, σ is the logic sigmoid function, i, f, o, and c are, respectively, the input gate, forget gate, output gate, and cell state vectors, all of which are the same size as that of the hidden vector h, and W are the weigh matrices.

The core of memory cell is the recurrently self-connected unit. The memory cells memorize the temporal state and control the information flow in the LSTM network by the three adaptive and multiplicative gating units. The input and outputs gate control the input and output activations into the memory cell, respectively. A forget gate is added to the memory cell to prevent the internal cell values from growing too large. It is realized by resetting itself once the information flow is out of date or by replacing the cell state with the multiplicative forge gate activation. By training the parameters in memory cells layer by layer, the LSTM network can store information and capture the complex correlation features in both short and long terms by the function of different gates. Therefore, the LSTM network can predict stress value in the next time step based on prior information without specifying the number of previous steps to be tracked back.

In the whole LSTM topology with input and output layers, the output forecast result is based on the internal computation of the memory cells in hidden layers. Therefore, the number of hidden layers and the number of LSTM memory cells in each hidden layer are the two key factors in modeling a LSTM network for fatigue load identification. Moreover, as higher-level modeling of input feature can make a LSTM network easier to learn temporal between successive steps [38], the selection of input

variations is of great importance to the performance of the LSTM network.

4.2. LSTM Network Training. The input and output data are normalized so that every element of the input and output vectors is in range from zero to one. Then, the most characterizing features of the observed input data are identified by an advanced feature selection method named RCDFS, in which relevance, redundancy, and redundancy-complementariness dispersion are taken into account to select the most effective subset from the measured vibration signals [39]. As a result, four input data, which are, respectively, the displacement of vehicle body in the z direction, the angular velocity of vehicle body in the x direction, and the deformation of two springs in the rear torsion beam suspension, are chosen as the maximum factors influencing the measured stress histories. Various LSTM networks are evaluated, varying along three main hyperparameters, the number of hidden layer (nh), the number of memory cells in each hidden layer (nc), and learning rate (α). During the training of various LSTM networks, weight parameters are updated by root mean square propagation (RMSprop) optimization method. The detailed execution steps are referred to in [40, 41]. For different stress histories at each critical position, the corresponding LSTM network is trained.

4.3. Determination of the LSTM Network. Different combinations of nh, nc, and α are used to obtain the best performance for the test data set. To achieve trade-off between training speed and convergence accuracy, nh is restricted in the range from 1 to 5, nc30 to 80. In the process of tuning these hyperparameters of the LSTM network, two findings are discovered: an improper setting can lead to a bad performance; nh is less important than other two hyperparameters. By trial and error, the final architecture of the LSTM network with the lowest error rate in the form of mean square error is achieved as shown in Figure 7. It can be found that the determined three main hyperparameters nh, nc, and α are 1, 40, and 0.5, respectively. Besides, the maximum number of epochs and the batch size are set to 1000 and 50, respectively.
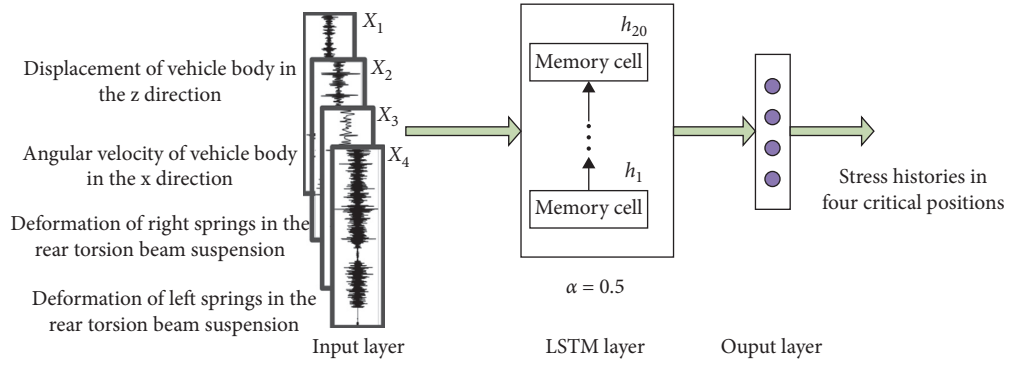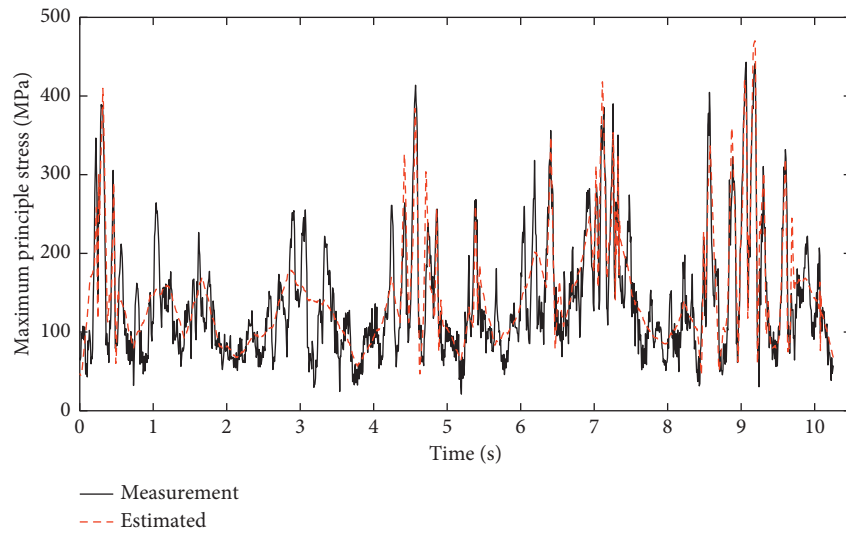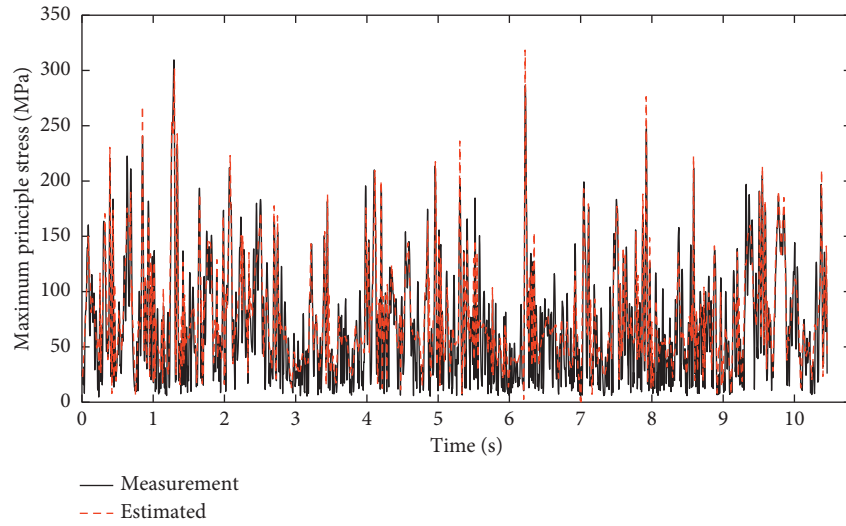
FIGURE 7: Final architecture of the LSTM used for stress histories estimation.
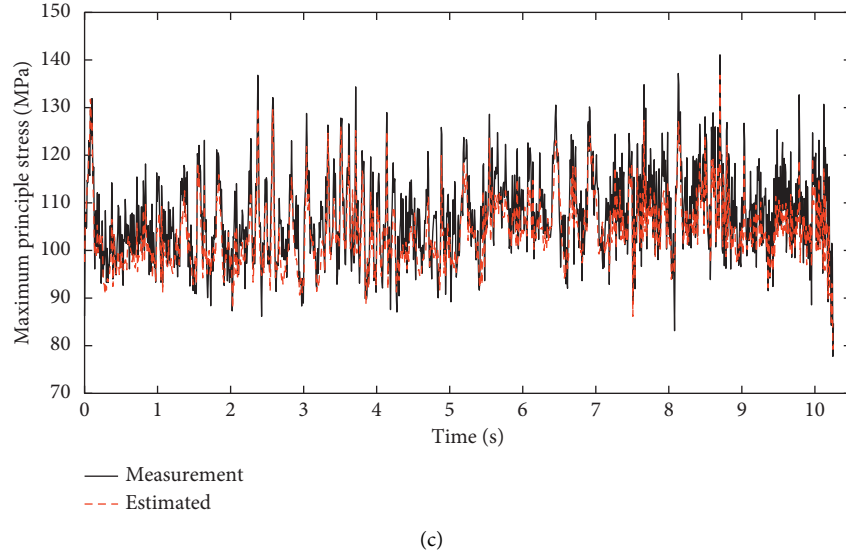

(a)

(b)

FIGURE 8: Continued.

(c)

FIGURE 8: Stress histories estimation performance comparison for measuring point 1. (a) Country road. (b) Pavement. (c) Highway.

TABLE 3: Performance of different models.

Category	Layer size	Point 1		Point 2		Point 3		Point 4	
		R^2	P (%)	R^2	P (%)	R^2	P (%)	R^2	P (%)
SVM	C - 1.2 G - 1000	0.52	−43.6	0.50	−46.9	0.52	−44.4	0.51	−45.9
BP	500–500	0.55	−41.8	0.54	−40.8	0.54	−42.3	0.54	−42.8
NARX	50	0.63	−21.2	0.59	−23.3	0.64	−22.6	0.60	−25.7
EKF		0.39	−81.4	0.43	−73.2	0.39	−77.9	0.41	−75.6
LSTM	40–40	**0.76**	**−17.1**	**0.78**	**−16.7**	**0.76**	**−16.9**	**0.75**	**−17.5**

5. Result Analysis and Comparison

The proposed LSTM network is validated by the use of collected data set from road tests. The predicted stress histories and the measurements are compared, and a short part of the results are shown in Figure 8. The comparison shows that the predicted stress histories have similar dynamic patterns with the measurements, close to the measurements. Two criteria are used to evaluate the performance of the proposed LSTM network: the dynamics and damage estimation accuracy of the predicted results in comparison with the measurements. The former is in the form of R-square (R^2) for the stress histories, and the latter in the form of deviation for the calculated damage value (P).where $\widehat{Y}_t$ are the predicted stress histories, Y_t are the measured stress histories, $\overline{Y_t}$ is the mean value of the measured stress histories, and D and $\widehat{D}$ are the damage value calculated by measured stress histories and predicted stress histories, respectively. The two criteria are chosen for two reasons. First, the predicted stress histories are used for damage calculation in our damage-oriented health monitoring system. Second, damage mainly reflects the entire distribution of stress histories, which can be revealed by R^2.

To validate the efficiency of the proposed LSTM network further, the performance of the LSTM-based identification method is compared with that of several methods using other representative models. In this paper, SVM, BP neural network, NARX neural network, and EKF are selected as comparison group. The hyperparameters of the four models are calibrated repeatedly to achieve their best performance in the same way as LSTM neural network. Specifically, for SVM and BP neural network, the input time lag is set to 3. Thus the dimensions of input variable are 12, including the four input variables of LSTM network in 3 consecutive time steps. In SVM, the best regularization parameters C and G are 1.2 and 1000, respectively. The determined BP neural network contains two hidden layers, and the number of neurons in the hidden layers is 100 and 50, respectively. In NARX neural network, the number of input delay is 3 and the two hidden layers both contain 30 neurons. The EKF model is built based on the application of unit load finite element analyses [42]. As a LSTM network can automatically calculate the optimal time lags, it does not need to specify time window size.

The models of the LSTM network and comparison group are programmed by MATLAB language. Based on the predicted stress histories for the validating data set, the performance of different models are shown in Table 3. The model with the best performance is marked in bold. It is clear that a LSTM network outperforms other models.

$$R^2 = \frac{\left(\sum_{t=1}^{n} \left(\widehat{Y}_t - \overline{Y}_t\right)^2\right)}{\left(\sum_{t=1}^{n} \left(Y_t - \overline{Y}_t\right)^2\right)},$$

(4)

$$P = \frac{\widehat{D} - D}{D} \times 100\%,$$

According to the comparison, the performance of the predicted results is the best with the use of a LSTM network, followed by NARX neural network, BP neural network, and SVM; the use of EKF is the worst. The EKF is obviously inferior to other intelligence approaches, which is caused by many hypotheses of statistical model in this model. The SVM shows weakness when compared with other deep learning networks. The NARX neural network and LSTM network, which are recurrent neural networks, show better performance than other models. Moreover, the memory cells enable the LSTM network to better capture nonlinear dynamics in long time term than other models.

Under real driving conditions, the structural health monitoring system estimates the damage value with the deviation of approximately 17% in comparison with measurements. In consideration of large data size, this result is satisfying. The major source of the error lies in the following aspect. The training data set is collected from limited driving cycles, while the data set to validate the LSTM neural network is fully random.

6. Conclusion and Future Work

In this paper, a novel health monitoring system based on a long short-term memory (LSTM) network is proposed to estimate the remaining fatigue life of automotive suspensions. The system applies a LSTM-based load identification method to predict sequential fatigue loads from available sensory signals. According to the comparison with other methods (SVM, BP, NARX, and EKF), the LSTM network can improve the accuracy in remaining fatigue life estimation. Furthermore, it is concluded that the LSTM network makes the proposed method effective and promising to capture nonlinear dynamics in large time-series sensory data. This research can inspire more studies in health monitoring of automotive components.

In the future, three major works are needed to make the health monitoring system more accurate and adaptive with higher robustness. Firstly, larger database, which contains experimental data set under more driving cycles, will be built. Secondly, the improvement of the proposed LSTM network or exploration of new algorithms is in our plan. For example, a combination of a LSTM network and a convolutional neural network has shown its advancement [43–45]. Thirdly, various uncertainty sources that affect the robustness of the monitoring method will be taken into consideration, such as the subtle structural differences among the same vehicles, the differences of dynamic stress responses in different life-span stages when the vehicle is under the same driving cycles, and uncertainty quantification of the predicted remaining fatigue life.

Data Availability

The figures and tables data used to support the findings of this study are included within the article.

Conflicts of Interest

The authors declare that they have no conflicts of interest.

References

[1] Y. Ling and S. Mahadevan, "Integration of structural health monitoring and fatigue damage prognosis," *Mechanical Systems and Signal Processing*, vol. 28, pp. 89–104, 2012.

[2] M. Gobbato, J. P. Conte, and J. B. Kosmatka, "Statistical performance assessment of an NDE-based SHM-DP methodology for the remaining fatigue life prediction of monitored structural components and systems," *in Proceedings of The IEEE*, vol. 104, no. 8, pp. 1575–1588, 2016.

[3] S. Kim, D. M. Frangopol, and M. Soliman, "Generalized probabilistic framework for optimum inspection and maintenance planning," *Journal of Structural Engineering*, vol. 139, no. 3, pp. 435–447, 2013.

[4] J. Z. Sikorska, M. Hodkiewicz, and L. Ma, "Prognostic modelling options for remaining useful life estimation by industry," *Mechanical Systems and Signal Processing*, vol. 25, no. 5, pp. 1803–1836, 2011.

[5] W. Fan and P. Qiao, "Vibration-based damage identification method: a review and comparative study," *Structural Health Monitoring*, vol. 10, pp. 83–111, 2011.

[6] A. Valencia, D. L. Fassois, and D. Spilios, "Damage/fault diagnosis in an operating wind turbine under uncertainty via a vibration response Gaussian mixture random coefficient model based framework," *Mechanical Systems Signal Processing*, vol. 91, pp. 326–353, 2017.

[7] C. H. Loh, K. J. Loh, Y. S. Yang et al., "Vibration-based system identification of wind turbine system," *Structural Control and Health Monitoring*, vol. 24, pp. 1876–1890, 2017.

[8] K. Maes, A. Iliopoulos, W. Weijtjens, C. Devriendt, and G. Lombaert, "Dynamic strain estimation for fatigue assessment of an offshore monopile wind turbine using filtering and modal expansion algorithms," *Mechanical Systems and Signal Processing*, vol. 76-77, pp. 592–611, 2016.

[9] S. Eftekhar Azam, E. Chatzi, and C. Papadimitriou, "A dual Kalman filter approach for state estimation via output-only acceleration measurements," *Mechanical Systems and Signal Processing*, vol. 60-61, pp. 866–886, 2015.

[10] J. Klemenc and M. Fajdiga, "Predicting smoothed loading spectra using a combined multilayer perceptron neural network," *International Journal of Fatigue*, vol. 28, no. 7, pp. 777–791, 2006.

[11] N. Gebraeel, M. Lawley, R. Liu, and V. Parmeshwaran, "Residual life predictions from vibration-based degradation signals: a neural network approach," *IEEE Transactions on Industrial Electronics*, vol. 51, no. 3, pp. 694–700, 2004.

[12] J. Rafiee, F. Arvani, A. Harifi, and M. H. Sadeghi, "Intelligent condition monitoring of a gearbox using artificial neural network," *Mechanical Systems and Signal Processing*, vol. 21, no. 4, pp. 1746–1754, 2007.

[13] F. Cadini, E. Zio, and D. Avram, "Model-based Monte Carlo state estimation for condition-based component replacement," *Reliability Engineering & System Safety*, vol. 94, no. 3, pp. 752–758, 2009.

[14] K. Liu, Z. Wei, and Z. Yang, "Mass load prediction for lithium-ion battery electrode clean production: a machine learning approach," *Journal of Cleaner Production*, vol. 289, p. 2021.

[15] M. Guo, L. Xie, SQ. Wang, and JM. Zhang, "Research on an integrated ICA_SVM based framework for fault diagnosis," in *Proceeding of the 2003 IEEE International Conference on Systems, Man and Cybernetics*, pp. 2710–2715, Washington, DC, USA, October 2003.

[16] A. Malhi, R. Yan, and R. X. Gao, "Prognosis of defect propagation based on recurrent neural networks," *IEEE Transactions on Instrumentation and Measurement*, vol. 60, no. 3, pp. 703–711, 2011.

[17] P. Baraldi, M. Compare, S. Sauco, and E. Zio, "Ensemble neural network-based particle filtering for prognostics," *Mechanical Systems and Signal Processing*, vol. 41, no. 1-2, pp. 288–300, 2013.

[18] S. Foulard, M. Ichchou, S. Rinderknecht, and J. Perret-Liaudet, "Online and real-time monitoring system for remaining service life estimation of automotive transmissions - application to a manual transmission," *Mechatronics*, vol. 30, pp. 140–157, 2015.

[19] Z. Zheng, W. Chen, X. Wu, C. Peter, Y. Chen, and J. Liu, "LSTM network: A deep learning approach for short-term traffic forecast," *Intelligent Transport Systems*, vol. 11, pp. 68–75, 2017.

[20] Y. Lecun, Y. Bengio, and G. Hinton, "Deep learning," *Nature*, vol. 521, no. 7553, pp. 436–444, 2015.

[21] S. Hochreiter and J. Schmidhuber, "Long short-term memory," *Neural Computation*, vol. 9, no. 8, pp. 1735–1780, 1997.

[22] F. Gers, *Long short-term memory in recurrent neural networks*, Ph.D thesis, University of Hannover, Hannover, Germany, 2001.

[23] A. Graves and A. rahman Mohamed, "Geoffrey Hinton, "Speech recognition with deep recurrent neural networks," in *Proceedings IEEE International Conference on Acoustics, Speech and Signal Processing*, pp. 6645–6649, Brighton, UK, May 2013.

[24] Z. C. Lipton, J. Berkowitz, and C. Elkan, "A critical review of recurrent neural networks for sequence learning," *Computer Science*, vol. 4, pp. 1–35, 2015.

[25] X. Ma, Z. Tao, Y. Wang, H. Yu, and Y. Wang, "Long short-term memory neural network for traffic speed prediction using remote microwave sensor data," *Transportation Research Part C: Emerging Technologies*, vol. 54, pp. 187–197, 2015.

[26] R. Zhao, J. Wang, R. Yan, and K. Mao, "Machine health monitoring with LSTM networks," in *Proceedings of the 10th International Conference on Sensing Technology*, Nanjing, China, November 2016.

[27] L. Guo, N. Li, F. Jia, Y. Lei, and J. Lin, "A recurrent neural network based health indicator for remaining useful life prediction of bearings," *Neurocomputing*, vol. 240, pp. 98–109, 2017.

[28] Y. Wu, M. Yuan, S. Dong, L. Lin, and Y. Liu, "Remaining useful life estimation of engineered systems using vanilla LSTM neural networks," *Neurocomputing*, vol. 275, pp. 167–179, 2018.

[29] A. Guo, A. Jiang, J. Lin, and X. li, "Data mining algorithms for bridge health monitoring: kohonen clustering and LSTM prediction approaches," *The Journal of Supercomputing*, vol. 76, no. 2, pp. 932–947, 2020.

[30] K. Liu, Y. Shang, Q. Ouyang, and W. D. Widanage, "A data-driven approach with uncertainty quantification for predicting future capacities and remaining useful life of lithium-ion battery," *IEEE Transaction on Industrial Electronics*, vol. 68, no. 2021, pp. 3170–3180.

[31] L.-H. Zhao, S.-L. Zheng, and J.-Z. Feng, "Failure mode analysis of torsion beam rear suspension under service conditions," *Engineering Failure Analysis*, vol. 36, pp. 39–48, 2014.

[32] S. H. Lin, C. G. Cheng, C. Y. Liao, J.-M. Chang, and Y. M. Wu, *Experiment and CAE Analyses for Suspension under Durability Road Load Conditions*, SAE 2006-01-1624, Warrendale, PA, USA.

[33] A. D'Andrea, C. Cappadona, G. La Rosa, and O. Pellegrino, "A functional road classification with data mining techniques," *Transport*, vol. 29, pp. 419–430, 2014.

[34] GB/T 12679-1990, *Motor Vehicles-Durability Running-Test Method*, GB/T 12679-1990, China, 1990.

[35] N. A. Kadhim, S. Abdullah, and A. K. Ariffin, "Effective strain damage model associated with finite element modelling and experimental validation," *International Journal of Fatigue*, vol. 36, no. 1, pp. 194–205, 2012.

[36] J. Deng, B. Maass, and R. Stobart, "Minimum data requirement for neural networks based on power spectral density analysis," *IEEE Transactions Neural Network*, vol. 23, pp. 587–595, 2012.

[37] B. Bertsche, *Reliability in Automotive and Mechanical Engineering*, Springer, Berlin, Germany, 2008.

[38] R. Pascanu, C. Gulcehre, K. Cho, and Y. Bengio, *How to Construct Deep Recurrent Neural Networks*, Computer Science, Tysons, VA, USA, 2014.

[39] Z. Chen, C. Wu, Y. Zhang et al., "Feature selection with redundancy-complementariness dispersion," *Knowledge-Based Systems*, vol. 89, pp. 203–217, 2015.

[40] A. Felix, "Gers, "Learning precise timing with LSTM recurrent networks," *Journal of Machine Learning Research*, vol. 3, pp. 115–143, 2002.

[41] H. Luo, M. Huang, and Z. Zhou, "Integration of Multi-Gaussian fitting and LSTM neural networks for health monitoring of an automotive suspension component," *Journal of Sound and Vibration*, vol. 428, pp. 87–103, 2018.

[42] J. Kang, B. Choi, H. Lee, J. Kim, and K. Kim, "Neural network application in fatigue damage analysis under multiaxial random loadings," *International Journal of Fatigue*, vol. 28, no. 2, pp. 132–140, 2006.

[43] N. Tara, "Sainath, Oriol Vinyals, Andrew Senior, Hasim Sak, "Convolutional, long short-term memory, fully connected deep neural networks," in *Proceedings of the IEEE International conference on Acoustics, Speech and Signal Processing*, pp. 4580–4584, Queensland, Australia, April 2015.

[44] F. Javier Ordonez and D. Roggen, "Deep convolutional and LSTM recurrent neural network for multimodal wearable activity recognition," *Sensors*, vol. 16, pp. 115–139, 2016.

[45] R. Zhao, R. Yan, J. Wang, and K. Mao, "Learning to monitor machine health with convolutional bi-directional LSTM networks," *Sensors*, vol. 17, no. 2, pp. 273–290, 2017.